Cassini-UVIS observation of dayglow FUV emissions of carbon in the thermosphere of Venus.

B. Hubert(1), J.-C. Gérard(1), J. Gustin(1), D.V. Bisikalo(2) , V.I. Shematovich(2) , and G.R. Gladstone(3).

1. Laboratoire de Physique Atmosphérique et Planétaire, Université de Liège, Belgium
   (17, Allée du 6 Août, Bât. B5c, B-4000 Liège, Belgium)

2. Institute of Astronomy of the Russian Academy of Sciences, Moscow, Russia
   (48, Pyatnitskaya street, 119017 Moscow, Russia)

3. Southwest Research Institute, San Antonio, TX, USA
   (6220 Culebra road, San Antonio, Tx 78228-0510, USA).

June 2012
Submitted for publication to ICARUS
(45 Pages, 11 Figures, 4 Tables)

Running head: Observation of CI-FUV dayglow emissions of Venus.

Corresponding Author :

B. Hubert

University of Liège, Laboratoire de Physique Atmosphérique et Planétaire,
Institut d'Astrophysique et de Géophysique,
17, Allée du 6 Août, Bât. B5c,
B-4000 Liège,
Belgium

Tel : +32 (0)4 366 97 27
Fax : +32 (0)4 366 97 11

e-mail : B.Hubert@ulg.ac.be

Abstract

We analyze FUV spatially-resolved dayglow spectra obtained at 0.37 nm resolution by the UVIS instrument during the Cassini flyby of Venus. The intensities of the ultraviolet multiplets of carbon at 126.1, 156.1 and 165.7 nm are determined using a least squares fit technique applied to all dayglow spectra recorded by UVIS along the Cassini track. These intensities are compared with the results of a full radiative transfer model of these emissions, that includes the known photochemical sources of photons and resonant scattering of sunlight. The carbon density profile of the Venus thermosphere has never been directly measured and is taken from a model. We find a serious disagreement between these observations and modeling that can be accounted for by applying a scaling factor to the carbon column. This needed scaling factor is found to increase monotonically with solar zenith angle, suggesting a possible photochemical origin to the disagreement, possibly involving the photochemistry of molecular oxygen to which the carbon density is highly sensitive.

Keywords: Venus, Atmosphere ; Ultraviolet observation ; Radiative transfer ; Photochemistry

1. Introduction

The presence of carbon atoms in the thermosphere of planet Venus has been established in the early seventies by *Rottman and Moos* (1973) using a rocket-borne FUV spectrometer, that measured the intensity of the CI-156.1 and 165.7 nm emissions to be ~2.4 and ~4.0 kR respectively. This discovery was later confirmed by the detection of the CI-165.7 nm line by the spectrophotometer of the Mariner 10 spacecraft (*Broadfoot et al.*, 1974) and by the presence of both spectral features in the FUV spectra recorded by the Orbiter Ultraviolet Spectrometer (OUVS) on board the Pioneer Venus (PV) spacecraft (*Stewart et al.*, 1979; *Paxton*, 1983, 1985).

Scientific analysis of these observations made it possible to address the study of the carbon photochemistry and density profile. Direct measurement of the vertical distribution of carbon has never been performed. However, the C density was estimated at high altitude (i.e. above the CO layer that contaminates the CI emission measurements due to its fourth positive emission) by *Paxton* (1985) using PV-OUVS observations of 156.1 and 165.7 nm emissions. Full understanding of the carbon vertical profile nevertheless remains an open question, and remote sensing of the carbon emissions is the most important source of observational constraints to guide its scientific investigation.

Excitation of the upper states of the 165.7 and 156.1 nm multiplets ($3s^3P^0$ and $2p^3D^0$ respectively) can mainly be achieved through photodissociation and dissociation by electron impact on the CO and CO_2 molecules, by direct electron impact on C atoms and by resonance scattering of photons (either solar or endogenous). Photodissociation of CO is the dominant mechanism producing ground state carbon, but dissociative recombination of CO^+ and CO_2^+

cannot be neglected, especially at high altitude (*Fox and Paxton*, 2005). It has already been established that the main sink of carbon in the thermosphere of Venus is the reaction

$$C + O_2 \rightarrow CO + O \qquad (1)$$

although the O_2 density profile has never been measured, and remains largely unknown. Several authors have developed elaborated models of the Venusian thermospheric and ionospheric photochemistry that now include the carbon photochemistry, making an assumption on the $f_{O_2} = [O_2]/[CO_2]$ mixing ratio (*Fox and Dalgarno*, 1981; *Fox*, 1982, 2003; *Fox and Bougher, 1991 and references therein; Paxton*, 1983; *Fox and Bakalian*, 2001; *Fox and Sung*, 2001; *Fox and Paxton*, 2005). Indeed, estimation of the carbon density combined with a detailed photochemical modeling is the only method available up to now to evaluate the O_2 density, which has never been measured directly. *Fox and Sung* (2010) calculated a carbon density profile too low compared with the results of *Paxton* (1985), that could be attributed to a too large value of f_{O_2}. *Fox and Paxton* (2005) used recent reaction parameters to re-investigate the carbon photochemistry and compare the results with the density profile of *Paxton* (1985) at high altitude. They estimated that $f_{O_2} \sim 3 \times 10^{-4}$. The knowledge of the carbon density profile is a key element in modeling and understanding the FUV carbon emissions. Full disc observation of the carbon emissions were also obtained by *Feldman et al.* (2000) using the Hopkins Ultraviolet Telescope (HUT) on Astro-2, who found 800 ± 27 R at 156.1 nm and 1500 ± 50 R at 156.7 nm. These numbers did however include the contribution of the blended CO (A-X) Fourth Positive emission blended with the carbon lines at the HUT resolution.

Scattering of the solar carbon UV lines largely dominates the total source of UV photons (*Fox and Paxton*, 2005 and references therein) but photochemical sources need to be included as well. Resonant lines of carbon, such as the multiplets at 156.1 and 165.7 nm, have large transition probabilities, so that a detailed model is needed to describe the multiple scattering and radiative transfer, that determine the intensity of the radiation field in the thermosphere.

New observations of the FUV and EUV emissions of Venus were obtained with the Ultraviolet Imaging Spectrograph (UVIS) (*Esposito et al.*, 1998) during the Cassini flyby of Venus. These data were used to study the Fourth Positive system of CO and the oxygen emissions at 130.4 and 135.6 nm by *Hubert et al.* (2010). These authors also determined the intensity of every spectral feature identified in the FUV spectra recorded by UVIS, using a least squares fit technique guided by spectroscopic constraints. They compared the observations with a model of the oxygen radiative transfer at 130.4 nm and with simple line of sight integration of the sources at 135.6 nm. The photochemical excitation rates used in that study were computed with the Monte Carlo model of *Shematovitch et al.* (2007), that had already been applied to the atmosphere of Venus by *Gérard et al.* (2008) and the radiative transfer was computed with the model of *Gladstone* (1985). They found a good agreement between observation and model results using the atmosphere from the VTS3 model (*Hedin*, 1983) and including the resonance scattering of the solar OI-130.4 nm line.

Gérard et al. (2010) studied several EUV features of the Venus ultraviolet spectra recorded by Cassini-UVIS and analyzed the OII 83.4 nm, OI 98.9 nm, Lyman-ß + OI 102.5 nm and NI 120.0 nm multiplets, and the CO C–X and B–X Hopfield–Birge bands. The calculated intensity variation of the CO B–X emission along the track of the UVIS slit was in fair agreement with the observations. They also found that the O, N_2 and CO densities from the empirical VTS3 model provide satisfactory agreement between the calculated and the observed EUV airglow emissions. However they found that the O^+ density obtained by extrapolating the model results of *Fox and Sung* (2001) versus F10.7 was too low to account for the observation. *Gérard et al.* (2011) also modeled the EUV HeI-58.4 nm emission of

Venus and compared their results with the observation of Cassini-UVIS. They again found that the observations are correctly reproduced by the model using the solar HeI-58.4 nm flux of the EUVAC model (*Richards et al.*, 1994) together with the helium density provided by the VTS3 model.

In this study, we present the intensity of CI- 126.1, 156.1 and 165.7 nm emissions recorded with the UVIS instrument along the track of the Cassini spacecraft during its flyby of Venus on 24 June 1999, on its way to Saturn. The radiative transfer of these emissions through the Venus thermosphere is modeled and compared with the observation in order to constrain the carbon density profile.

2. Observations

The Cassini spacecraft was launched on 15 October 1997. On its long journey to Saturn, the spacecraft took a gravitational assist to gain energy from Venus on 24 June 1999. The UVIS instrument on board Cassini (*Esposito et al.*, 1998) obtained a series of FUV spectra during this flyby, at a time period of rising solar activity, when the F10.7 solar index was ~214 at Earth distance. During the flyby, Cassini reached an altitude of closest approach of 602 km. The spacecraft had to be oriented so that its 4-meter antenna shielded the payload from the Sun. This required UVIS to look in a direction nearly perpendicular to the Sun-spacecraft line, so that the phase angle remained close to 90°. The foot track of the flyby was detailed by *Hubert et al.* (2010) and *Gérard et al.* (2011). A total of 55 records of 32 s have been obtained along the track at a 0.34 nm spectral resolution. Twenty-two of them showed dayglow emissions, as the UVIS field of view intersected the illuminated disc of Venus.

The intensities of the many spectral features present in the FUV-UVIS channel were determined using the least squares fit technique developed by *Hubert et al.* (2010). The carbon lines that we want to study here are blended with emissions of the CO 4th positive system at the UVIS resolution. Instead of using deconvolution or a limited well choosen set of spectral features of known Franck-Condon factors to try to separate the different emissions present in the UVIS pass-band, our least squares fit technique constrains the relative intensity of all the CO-4P emissions having a common upper state using the Einstein transition probabilities of the CO-4P bands that are deduced from the results of *Kurucz* (1976), thus including all the Franck-Condon factors of the CO-4P system at once. However, as noted by Hubert et al. (2010), the intensities of the (v',0) bands can be self-absorbed. The least-squares fit method was thus designed as to determine the (v',0) emissions separately, without constraining it by the Einstein transition parameters (that include the Franck-Condon factors). The least squares fit technique thus presents the advantage of including the additional spectroscopic information which would not be accounted for by a deconvolution technique, while it also accounts for all the relevant spectral data and spectroscopic constrains at once to determine the needed intensities, which would not be guaranteed by a simple method using the expected relative intensity of a few, well chosen, CO-4P bands. **Figure 1** shows the observed and fitted intensities obtained for UVIS record 25, i.e. for the observation having the smallest possible emission angle along the Cassini track. Panel a shows that the observed spectrum is well accounted for by the fitted spectrum between 125 and 180 nm. Panel b shows the contributions of the CO fourth positive system (black), oxygen multiplets (red) and carbon multiplets (greed, from CI and CII transitions) to the fitted spectrum. In particular, the CI multiplets at 156.1 and 165.7 nm are detailed in panels c and d, that show that the corresponding observed spectral features are well represented by the fitted spectrum, that includes contributions from both the CO-fourth positive system and the CI multiplets. **Table 1** lists the transitions of main interest that were identified in the FUV channel between ~125 and ~180 nm, and included in the fitting process. Although the carbon emissions at ~114.1, 115.8, 119.4 and ~127.8 nm are present in the UVIS pass band, they were not analyzed in details due to the presence of a large number of unresolved line blends between carbon transitions and with emissions from other atoms as well. For example, more than 20 spectral lines of carbon exist between 127 and 129 nm (*Reader et al.*, 1980, *Weise and Fuhr,* 2007). **Figure 2** shows the intensity variation of the brightest CI and CII lines included in the fitting of the UVIS FUV spectra between ~125 and ~180 nm. The CI transitions at 143.2 and 146.3 nm (not shown in **Figure 2**) involve two excited states, and are found to have a negligible intensity in the Venus spectra. As it appears in Figure 1 and in Figure 2 of *Hubert et al.* (2010), the CI-132.9 and CII-133.5 nm multiplets form a single broad feature in the UVIS pass band, and it is hard to determine whether the fitted intensities are fully reliable, despite the small uncertainties deduced from Poisson noise propagation and chi-square function flatness given in **Figure 2**. As already mentioned, the CI – 127.8 nm signal results from the accumulation of many multiplets. The apparently large intensity of the 127.8 nm feature does thus not warranty that one of the multiplets is very bright itself. Moreover, this spectral interval is so crowded with transitions that obtaining the solar intensity necessary for a detailed modeling is at least challenging. This spectral feature is thus not suitable for further theoretical analysis. The brightest multiplets at 156.1 and 165.7 nm have already been used by other authors to study the thermosphere of Venus (*Paxton*, 1985 for example). The large brightness of these lines and the absence of other carbon multiplets at near wavelength make them ideal tools for theoretical analysis. On the other hand, the CI – 126.1 nm transition is much weaker and has much larger uncertainties, as it obviously appears in Figure 1. However, this spectral feature is well isolated at the UVIS resolution and will also be included in the simulations.

3. Photochemical model.

The Monte Carlo model of *Shematovitch et al.* (2010) solves the Boltzmann equation for the ionospheric electrons of planet Venus using a stochastic method. The electrons can be produced by solar EUV photons ionizing the neutral constituents of the Venus thermosphere. Secondary electrons can also be produced by collisions between already present electrons with atoms and molecules of the gas. The model computes the energy degradation of the photoelectrons and secondaries to obtain the energy distribution function of the electrons. The rate of electron impact-production and excitation of the upper state of atomic and molecular transitions relevant to aeronomic observations are then calculated using relevant cross sections. The photochemical sources of excitation of those transitions are thus computed and made available for further radiative transfer treatment (or simple line-of-sight integration under optically thin conditions). The radiative transfer model must however also include resonance scattering of the solar radiation, which is the dominant primary source of CI photons in the thermosphere (*Fox and Paxton*, 2005). The photochemical excitation processes accounted for in our modeling of the CI 126.1, 156.1 and 165.7 nm emissions are

$$\begin{cases} CO + h\nu \rightarrow C^* + O \\ CO + e \rightarrow C^* + O + e \\ CO_2 + h\nu \rightarrow C^* + 2O \\ CO_2 + e \rightarrow C^* + 2O + e \\ C + h\nu \rightarrow C^* \\ C + e \rightarrow C^* + e \end{cases} \tag{2}$$

The photodissociation cross sections of CO_2 and CO producing the CI 3s $^3P^0$ and CI 2p^3 $^3D^0$ are taken from *Wu et al.* (1978) and *Wu and Judge* (1981). The photodissociative excitation cross sections of CO and CO_2 are not known for the CI 3d $^3P^0$ state, and this process has been ignored in the model. Electron impact on CO can produce CI excited in the 3s $^3P^0$, 2p^3 $^3D^0$ and 3d $^3P^0$ states. The cross sections for the 165.7 and 156.1 nm emissions were obtained by scaling that of the CI-128 nm emission (*Paxton*, 1985), with a factor based on the oscillator strength of these transitions (*Goldbach and Nollez*, 1987). The cross section of *Ajello* (1971 a) at 127.8 – 128.0 nm has been scaled according to the oscillator strength for the 3d $^3P^0$ state. For the electron impact on CO_2, the energy dependent cross section for the excitation of the CI 127.8 – 128.0 nm emissions is scaled to the values at 100 eV for the 3s $^3P^0$ and $2p^3$ $^3D^0$ states (*Ajello* 1971 a,b; *Shirai* 2001). The cross section for the 3d $^3P^0$ state was scaled from the CI 127.8 – 128.0 cross section according to the oscillator strength. Direct excitation of carbon atoms by electron impact were included using the cross sections of *Dunsheath* (1997) for the three 3s $^3P^0$, $2p^3$ $^3D^0$ and 3d $^3P^0$ states.

The carbon density profile was obtained by scaling the low and high solar activity density profiles of *Fox and Paxton* (2005) by the $F_{10.7}$ index. **Figure 3** shows the carbon density profile and the calculated photochemical excitation rates of the 126.1, 156.1 and 165.7 nm upper states of carbon, for the condition of the UVIS record number 25, which has the most vertical viewing direction of the flyby, and a solar zenith angle SZA= 64.23 deg. For the transition at 126.1 nm, photodissociation of CO and CO_2 is neglected, the cross sections of these processes remaining unknown for the CI 3d $^3P^0$ channel. Around 150 km of altitude, electron-impact dissociation of CO and CO_2 have magnitudes comparable to that of the direct impact of electrons on carbon atoms, which becomes the dominant source above 160 km. Electron-impact dissociation of CO_2 dominates below 135 km of altitude. Several local maxima appear below the main peak as a consequence of the complex interplay between the density profile of the dominant species, and the altitude-dependent absorption of solar ultraviolet and solar X rays emissions that control the photoelectron source. This remark holds as well for the excitation of the CI-156.1 nm transition, which is mostly dominated by the electron-impact dissociation of CO_2, at nearly all altitudes. The other processes are nevertheless not negligible photochemical sources. The photochemical excitation of the CI-165.7 nm transition is dominated by the electron-impact dissociation of CO_2 below 135 km, whereas at higher altitude, this source becomes comparable with (and sometimes smaller than) the photo-dissociation of CO_2. It is important to note that all dissociative excitation processes are exothermal reactions. As a result, the produced fragments and thus the produced carbon atoms, mostly have a speed well above the thermal speed. This means that thermospheric thermal carbon atoms have a small probability of scattering photons emitted by those newly produced fast carbon atoms. The way to handle these emissions (produced by the fast carbon atoms) is thus to neglect all radiative transfer effect on them, and to consider that the thermosphere of Venus is optically thin to these photons, so that a direct line of sight integration of the calculated emission rate is needed to simulate the contribution of these nonthermal sources of photons to the observed Cassini-UVIS intensity. Only the direct electron impact excitation of thermospheric carbon atoms may require a detailed radiative transfer calculation. This source peaks close to the maximum of the carbon density (2.6×10^6 cm^{-3}) shown in **Figure 3d**. The density profile of CO_2, the most important constituent of the thermosphere of Venus, is also shown for comparison.

4. Radiative transfer modeling.

The photochemical sources described above must not all be included in a full radiative transfer modeling of these emissions, as explained above. Only the direct electron impact excitation of carbon atoms is concerned by this paragraph. The carbon density is so low in the thermosphere of Venus that optical thickness is not very large at these wavelengths. Including a full radiative transfer modeling is nevertheless more accurate, especially for slant views of the thermosphere, such as for the observing conditions of Cassini-UVIS. Moreover, this allows us to conduct consistent sensitivity tests on the carbon density profile, such as those that we will make to constrain the carbon density profile.

A full treatment of the radiative transfer of the carbon emissions at 126.1, 156.1 and 165.7 nm must include scattering of the solar emissions at these wavelengths. *Shine et al.* (1978) have measured the solar spectrum at 156.1 and 165.7 nm at a very high resolution, resolving the line shape of every line of both multiplets. The solar spectrum reveals strongly reverted broad lines that overlap each other. Fortunately, the temperature of the Venus thermosphere is sufficiently low to neglect these overlaps in the radiative transfer treatment, all lines being separated from each other by many Doppler widths. However, the detailed shape of the solar spectrum cannot be neglected. The radiative transfer model of *Gladstone* (1985) assumes line shapes symmetrical about the line center, which can be approximated by the sum of two symmetrically shifted Gaussian functions of same width and magnitude. These Gaussian functions can be described in terms of two parameters x_{dis} and x_{off} that quantify the dispersion of both Gaussians and their offset with respect to the rest wavelength, expressed in standard Doppler units at a suitable temperature, as it was previously done by *Gladstone* (1992) for the solar OI-130.4 nm multiplet. The model solves the radiative transfer for the red-shifted wing, thus neglecting any difference between blue-shifted and red-shifted photons. This approximation is fully satisfying in planetary atmosphere, but the non-symmetrical, blended line shapes measured by *Shine et al.* (1978) cannot be used in the model without adaptation. We constructed symmetrized line shapes about every line of both multiplets that can be approximated using two Gaussian functions. We ensured that the input flux at line center was compatible with the actual non-symmetric line shape, so that formally, blue-shifted and red-shifted photons can be considered as equivalent in the radiative transfer treatment, i.e. that the wavelength-symmetrized radiative transfer produces the same intensity as a full non-symmetrized treatment would do. For the CI-126.1 nm multiplet, the contribution of each line of the multiplet to the solar flux was determined by fitting the SOHO-SUMER spectrum (*Curdt et al.*, 2001) using Gaussian functions. We found that the relative contributions are

0.018, 0.123, 0.007, 0.289, 0.417 and 0.146 at 126.0927, 126.1122, 126.1552, 126.0735, 126.0996 and 126.1426 nm respectively.

The total absolute flux of the solar multiplets are estimated as follows. First, the relative contribution of each multiplet to the solar intensity of a broad wavelength interval is estimated using the SOHO-SUMER spectra of *Curdt et al.* (2001). Second, the integrated solar flux of the same wavelength interval is estimated for the observing conditions prevailing during the Cassini flyby using the empirical model of *Woods and Rottman* (2002), which is based on an $F_{10.7}$ proxy. The flux of each multiplet is then estimated considering the multiplet contributes to the solar spectrum in the same proportion as that found using the spectrum of *Curdt et al.* (2001). This method allows us to estimate the solar flux of each multiplet for any solar activity, and in particular for the conditions of the Cassini flyby (assuming that the ratios that we estimate are not activity-dependent), despite the lower spectral resolution used by *Woods and Rottman* (2002). The relative contributions of the CI sextuplets to the solar flux are summarized in **Table 2**.

Table 3 lists the transition parameters used in the present study. The parameters x_{dis} and x_{off} refer to the dispersion and offset of both Gaussian functions relevant to each line in the observed solar spectra symmetrized about the rest wavelength of each particular line. As the detailed high resolution solar spectrum remains unknown for the CI-126.1 nm multiplet, the values of the x_{dis} and x_{off} parameters are assumed equal to the average of all the transition of the CI-156.1 and 165.7 nm multiplets. CI lines in **Table 3** are grouped by upper state, because the radiative transfer of transitions having a common upper state must be treated in a coupled manner. Each multiplet can thus be decomposed into a singlet, a doublet and a triplet of coupled lines. The solar flux relevant of each multiplet, deduced from the model of *Woods and Rottman* (2002) following the procedure described above, needs to be scaled to account for the distance between the Sun and Venus. The $F_{10.7}$ index used in the solar flux proxy accounts for the Earth-Sun-Venus angle. For comparison, the solar fluxes obtained by integrating the SOHO-SUMER spectrum of *Curdt et al.* (2001) (obtained for different activity conditions), across the wavelength interval of the multiplets after removing the background, are 1.59 x 10^{10} cm^{-2} s^{-1} at 165.7 nm, 5.30 x 10^{9} cm^{-2} s^{-1} at 156.1 nm and 9.05 x 10^{7} cm^{-2} s^{-1} at 126.1 nm. Observations from the Solar EUV Experiment (SEE) instrument onboard the Thermosphere Ionosphere Mesosphere Energetics and Dynamics (TIMED) satellite (*Woods et al.*, 2000) can equally be used to estimate the solar flux at 156.1 and 165.7 nm for observing conditions similar to those of the Cassini flyby. The flux at 126.1 nm cannot be retrieved from the TIMED-SEE data, apparently due to the presence of the nearby solar Lyman-α line. We selected SEE solar spectra observed for $F_{10.7}$ ranging between 211 and 217, and we found 8 such observations. The average fluxes computed from these data are 1.80 x 10^{10} cm^{-2} s^{-1} at 165.7 nm and 4.60 x 10^{9} cm^{-2} s^{-1} at 156.1 nm. Reminding that the solar irradiance given by the model of *Woods and Rottman* (2002) is considered to be accurate within ~20%, all these fluxes are compatible with each other. The wavelengths and Einstein transition parameters listed in **Table 3** are from *Froese Fischer* (2006). The CO_2 polarisability of *Nir et al.* (1973) was used to compute the Rayleigh scattering cross sections with the formula given by *Thomas and Stamnes* (1999). The photochemical excitation rates shown in **Figure 3** are distributed among the sublevels of the carbon upper state proportionally to the degeneracy of each sub-state of the upper state. This is acceptable considering that the sub-states of a given electronic upper state only differ by their angular momentum, so that they have very similar energies.

Radiative transfer of the photons of photochemical and solar origins can be calculated separately, the results being summed up eventually for comparison with the observation. **Figure 4** shows the source functions of the CI-165.7 nm multiplet evaluated for the observing conditions of Cassini-UVIS record number 25, resulting from resonance scattering of the ultraviolet sunlight. The primary source represents the rate of introduction of photons in the thermospheric gas. It has two origins in the present model: the number of photons emitted per unit volume and per second by excited carbon atoms produced by the mechanisms listed in equations (2) on the one hand, and by resonance scattering of incident solar photons on the other. As already pointed out before, both can be treated separately. The primary source must not be confused with the source function of radiative transfer, which includes multiple scattering of photons in (resonance) transitions. Formally, the radiative transfer (RT) source function is equal to the number of atoms that emit a photon per second in a unit volume. The RT source functions of the doublet and the triplet include the effect of branching between lines having the same upper state. Both the primary sources and RT source functions include a wavelength and angular dependence which does not appear in **Figure 4**, that shows the wavelength and angle-integrated primary source and RT source functions. When the atmosphere is optically thick with respect to the studied emission, the RT source function can be several orders of magnitude larger than the primary source function of that emission. In contrast, both are equal in a perfectly optically thin case. As it can be seen in **Figure 4**, the Venus thermosphere appears as nearly optically thin when the carbon density profile of *Fox and Paxton* (2005) is used, despite the very large Einstein transition parameters of the multiplet lines (**Table 3**).

The radiative transfer source function of the solar photons presents its main peak around 140 km, around the maximum of the carbon density profile. A secondary peak occurs at lower altitude, corresponding to Rayleigh scattering of solar photons by CO_2. Such a situation is uncommon in the radiative transfer of resonance emissions through planetary atmospheres. It happens here because the carbon density is so low in the Venus thermosphere compared with that of CO_2 that Rayleigh scattering by CO_2 still plays a (minor) role despite its tiny cross section. Our result may however be biased by our use of a symmetrized line profile for each transition, so that the total solar flux including the far wings of the symmetrized solar input may differ from the actual solar input. We verified that ignoring the Rayleigh scattering in the radiative transfer of all the carbon multiplets does not significantly change our results and analysis concerning the observed and modeled Cassini-UVIS intensity (see below). Indeed, the Rayleigh peak is more than an order of magnitude smaller than the resonance peak, and it extends across a smaller altitude range, so that it represents a source of photons much smaller than resonance scattering of the solar line. Comparing with **Figure 3c**, it appears that scattering of sunlight dominates the photochemical sources of photons, as was previously pointed out by *Fox and Paxton* (2005). The column-integrated sources are listed in **table 4**. At 165.7 nm, the resonance scattering of solar photons dominates photochemical sources by nearly a factor 4. **Figure 5** shows the primary source and the radiative transfer source functions of the CI-156.1 nm multiplet. Comparing with **Figure 3b**, we notice that the solar source provides again the most important input of photons for this multiplet, although the magnitude of the solar flux at 156.1 nm is about three times smaller than that at 165.7 nm (**Table 3**). After column integration (**Table 4**) we find that the solar source of photons dominates the photochemical processes by more than a factor 3. The Rayleigh scattering also produces a secondary peak in the source functions, around ~120 km of altitude. The source functions of the CI-126.1 nm multiplet are shown in **Figure 6**. The source functions are lower than that of the CI-156.1 and CI-165.7 nm multiplets mainly because the solar flux is lower. In this case, resonance scattering of the solar line is largely dominated by the non-thermal photochemical sources of photons (which are optically thin) shown in **Figure 3a**. After column integration, the resonance scattering of the solar 126.1 nm photons only contribute ~7% of the total.

The radiative source functions are not directly observable. The CI-165.7 nm intensity computed along the Cassini track for the UVIS observing conditions are shown in **Figure 7a**. Our simulations are expected to be less accurate near the terminator and near the limb. As it could be expected based on the source functions, scattering of solar photons is the most important radiative process at 165.7 nm. Clearly, the simulated intensity is by far too low compared with the observation. The discrepancy increases at larger solar zenith angles, where the intensity is higher. In principle, the uncertainties affecting the fitted observed intensity should decrease as the signal to noise ratio decreases. We thus rule out a possible misidentification of the CI-1657 nm intensity as the origin of the discrepancy. Indeed, our fitting procedure has revealed efficient for several other emissions (*Hubert et al.*, 2010) such as the fourth positive band system of CO and the oxygen emissions at 130.4 and 135.6 nm. In our view, this discrepancy can have two origins: a too small solar flux, or a too low carbon density. We verified that the solar flux used in the present computation is reasonable by comparing it with the flux observed by the TIMED satellite at similar solar activity. The carbon density profile thus appears as the principal candidate for explaining the discrepancy. We conducted sensitivity tests by multiplying the carbon density profile of the model by factors ranging between 0.1 and 20. The CI-165.7 nm intensity computed along the Cassini track is shown in **Figure 7a** for several of them. The correction factor to be applied to the carbon density profile changes along the Cassini track. This point will be discussed again later. **Figures 7b and c** show the simulated and observed CI-156.1 and 126.1 nm intensities along the Cassini track. The same trends appear for these multiplets as for the CI-165.7 nm multiplet. Resonance scattering of the solar flux produces the main contribution to the 156.1 nm intensity while photochemical sources provide most of the 126.1 nm photons. However, the observed intensity at both wavelengths is much larger than that calculated using the carbon density profile of *Fox and Paxton* (2005), the discrepancy is more severe at larger SZA and increasing the carbon density may account for the discrepancy, the scaling factor to be applied being larger at smaller SZA.

The sensitivity of the 165.7, 156.1 and 126.1 nm intensities to the correction factor applied to the carbon density are shown in **Figure 8**, for the conditions prevailing for UVIS record 25. The response is clearly non-linear for the 156.1 and 165.7 nm multiplets. For small carbon densities, i.e. small correction factors, the response is fairly linear because the carbon column is optically thin for the photons of the CI-resonance transitions, and because none of the photochemical sources has a nonlinear dependence versus [C]. But, as the density is increased, the atmosphere becomes optically thick, and the sensitivity of the FUV intensity versus the carbon density decreases. This is intuitively natural: for a strongly optically thick medium, the solar radiation penetrates down to the altitude where the optical depth τ roughly equals 1. This altitude is wavelength-dependent, and it can be located rather deep in the atmosphere due to the large broadening of the (reverted) solar lines. The photons are thus absorbed at altitudes where the optical thickness at line center is very large, and the scattered solar photons enter the process of optically thick radiative transfer with multiple scattering. It also follows that, for a very optically thick atmosphere, multiplying the scatterer density by a factor e ~ 2.72 is more or less equivalent to simply rising the $\tau = 1$ altitude by 1 scale height, leaving the rest of the radiative transfer process nearly unchanged. One can thus expect that, under optically thick conditions and when the main source of photons is the solar input, the dependence of the observed intensity versus the scatterer density will remain weak, because most of the solar photons are scattered anyway, so the progressive loss of sensitivity versus the scaling factor shown in **Figure 8a,b**. The sensitivity of the CI-126.1 nm emission has a different dependence than that of the two other multiplets. Absorption of solar radiation plays a minor role for this emission. When the carbon density is low, the non-thermal photochemical sources of excited carbon provide the dominant source of photons, but when the carbon density is increased, the production rate of excited carbon by electron impact is similarly enhanced and progressively becomes the dominant primary source of photons, to which the Venus thermosphere also progressively becomes optically thick.

The correction factor to be applied to the carbon density profile to account for the Cassini-UVIS observation has been computed for the three multiplets, for all the UVIS observation of the dayglow along the Cassini track. **Figure 9** summarizes these results. The error bars represent the 1-σ uncertainty, estimated using the sensitivity of the computed intensity versus the carbon correction factor and the uncertainties on the observed intensities deduced from our fitting procedure. These uncertainties include the Poisson noise of the data and the effect of the flatness of the chi-square function. The values computed at SZA ~ 11° are obtained for a slant view of the planet limb, where our model may be less reliable. The last point of the CI-165.7 nm curve may thus not be reliable. The correction factors deduced from the three multiplets are roughly compatible with each other, especially at SZAs larger than 40° where they perfectly agree considering the uncertainties of the results. The reason why the correction factor deduced from the CI-156.1 nm strongly departs from that based on the CI-165.7 and 126.1 nm multiplets at SZA > 40° remains unclear. However, our analysis suggests that the carbon density of the Venus thermosphere increases at smaller solar zenith angle. This is apparently logical: a smaller SZA implies a larger incident solar flux, which increases ionization and photo-dissociative processes. One may speculate that a larger SZA leads to a larger production of carbon atoms by dissociation of carbon-based molecules, and to an inccrease of the O_2 loss rate due to photo-dissociation of that molecule by solar UV radiations. In parallel, the production of O_2 by photodissociation of CO_2 is increased in similar proportion (neglecting the variation of the CO_2 density versus SZA). An increased solar UV flux would also increase the production of oxygen atoms, that can recombine and form O_2 molecules in three-body collisions. Triple collisions are slow processes, and in addition, the general thermospheric circulation of Venus is characterized by a Hadley cell that transports the produced oxygen atoms from the day to the night side, especially at small SZA, thus reducing the production rate of O_2 molecules by that process. We thus do not expect that the O_2 mixing ratio would be largely dependent on SZA, because a variation of the solar flux would similarly impact the loss and main production rates of O_2, leaving the equilibrium concentration nearly unchanged. A smaller SZA could thus imply a larger production rate and an unchanged loss rate of carbon atoms, and consequently a larger carbon concentration as suggested by the observations. A complete three-dimensional modeling of the coupled photochemistry and general circulation of the thermosphere of Venus would be necessary to establish if our proposed speculation is the actual reason of the SZA dependence that we find for the carbon density.

The density profile of *Fox and Paxton* (1985) was computed for a SZA=60°, adjusting the O_2 density profile to match the carbon density profile deduced by *Paxton* (1985). We find that a factor ~6.5 must be applied to the carbon profile to account for the observation near SZA = 60°. Our observation and modeling thus suggest a discrepancy with the carbon density profile deduced by *Paxton* (1985), which stems from the larger solar flux used by *Paxton* (1985). The carbon density deduced from *Paxton* (1985) puts a constrain on oxygen to carbon dioxide ratio to be $[O_2]/[CO_2] \sim 3 \times 10^{-3}$. For comparison, the model of *Krasnopolsky and Parshev* (1983) had $[O_2]/[CO_2] \sim 6 \times 10^{-4}$ at ~140 km of altitude, that would produce a 5 times lower carbon loss rate due to reaction (1) and thus a five times larger carbon density, providing that the production rate of carbon would remain unchanged. Such a factor is roughly what we find around SZA = 60°.

The brightest emission being the CI-165.7 nm multiplet, one could expect that the correction factor estimated based on this emission would be the most reliable. However, the response of the calculated intensity versus the carbon density is slightly more non-linear. The computed 165.7 nm intensity is, in principle, less sensitive to the carbon density than that of the other multiplets, at least when the carbon density is largely increased and the optical thickness becomes significantly larger than 1. The 126.1 nm emission, as it is modeled in this study, mostly depends on the electron impact excitation of carbon atoms, which is directly proportional to the density, but its low intensity produces larger uncertainties. In addition the detailed line profile of the 126.1 nm solar multiplet is unknown, introducting an additional source of uncertainties. It is thus difficult to determine which of the three multiplets is the best suited for estimating the correction to be applied to the carbon density profile. The very different results found at larger SZA values between the 156.1 and 165.7 nm – determined scaling factors indicate that some elements still escape our understanding of the carbon density profile (unless it would result from uncertainties on the fitted intensities). One possibility would be that the shape of the carbon density profile, not only the (peak) absolute value, would need to be revised. This could suggest that a part of the processes governing the photochemistry of carbon remains misunderstood. For example, does transport play any role? Are all the photochemical cross sections sufficiently well known, etc. ? Indeed, the SZA-dependence of the needed correction factor clearly points to a photochemical origin of the discrepancy between the observed and computed intensities, as already explained before.

An observational origin of the discrepancy between the multiplets must also be considered. The reason why different correction factors are found based on the CI-156.1 and 165.7 nm emission is illustrated in **Figure 10a**, which shows the ratio between the Cassini-UVIS CI-156.1 and 165.7 nm intensities. This ratio remains fairly stable for SZA > 40°, but it starts increasing at smaller SZAs. The ratio that we compute compares well with the value of ~0.5 of *Feldman et al.* (2000) who observed the FUV spectrum of the Venus disk using the Hopkins Ultraviolet Telescope (HUT), but who did not resolve the blend with the CO Fourth Positive band system. However, the tendency found for SZA < 40° points to a consistent, regular increase despite the uncertainties on the intensity ratio. By contrast, the CI-126.1 / CI-

165.7 nm intensity ratio remains stable over the whole Cassini-UVIS track. One could argue that the fitted intensity of the multiplets shown in **Figure 2** would have uncertainties larger than that estimated from the Poisson noise and chi square flatness because of the blend with the CO fourth positive band system at the UVIS wavelength resolution. This could be the reason of the different scaling factors that we deduce for the carbon density based on the CI-165.7 and 156.1 nm intensities at SZA < 40°. It nevertheless remains that, at smaller SZA values, the results found for the three multiplets consistently show that the carbon density profile must be significantly increased by a factor up to ~10 to account for the observations. In addition, the fitted intensity profiles shown in **Figure 2** have the same shape, and mostly differ through the magnitude of the intensity scale. After scaling to unitless values (by dividing each curve by its average along the track, for example), all the so-obtained relative intensities appear nearly superimposable, as shown in **Figure 11**. Even the relative intensity of ionized carbon does only slightly differ from those of atomic carbon multiplets. It naturally follows that all these emissions share a similar SZA-dependence. This is understandable because the ultraviolet solar flux at the top of any atmospheric column strongly drives all the photochemical processes in that column at day time. Fitting a line through the estimated carbon scaling factors (including the three emissions), we could verify that the discrepancy between low SZA values rather appears as a dispersion around the fitted line: indeed, including values for SZA above 39 Deg or not gives nearly the same fitted lines. The natural conclusion then remains that the carbon density profile varies versus SZA at a nearly linear rate that can be fitted for the Cassini flyby to ~-0.23 Deg^{-1}. It would thus also appear natural to infer from the observation that the carbon photochemistry of Venus is nonlinearly sensitive to the solar input. Further detailed modeling of the photochemistry of the thermosphere of Venus, including the mixing ratio of O_2, will be needed to understand that sensitivity.

5. Conclusion

The dayglow intensity of the CI multiplets at 126.1, 156.1 and 165.7 nm has been measured and spatially resolved across the Venus disc using the UVIS instrument during the Cassini flyby of the planet. The intensity of these emissions has been modeled including photochemical sources and resonance scattering of solar radiation. The carbon density profile was taken from the model of *Fox and Paxton* (1985). We find that the ratio between the observed 156.1 and 165.7 nm is compatible with previous observations obtained with the HUT instrument. A significant discrepancy is found between the observed and modeled intensity of the three multiplets, that we attribute to a too low carbon density. The scaling to be applied to the carbon density profile to account for the observations of the three multiplets consistently varies from ~2 at SZA~80° to ~10 for SZA~45°. At smaller SZA values, the 156.1 nm emission suggests scaling factors reaching as much as 20 while the 126.1 and 165.7 nm multiplets indicate scaling factors around 12. This internal discrepancy between emissions remains to be explained and appears as a scatter around a mostly linear dependence. All three analyzed multiplets nevertheless show a clear agreement at larger SZAs that points to a photochemical origin of the SZA dependence that we find for the carbon density in the thermosphere of Venus. The larger carbon density that we infer from the Cassini-UVIS FUV data also implies that the mixing ratio of O_2 is lower than previously thought, but this ratio does not necessarily need to vary versus SZA to account for the observations.

Aknowledgements. This study is based on observations by the Cassini project. B. Hubert and J.-C. Gérard are supported by the Belgian National Fund for Scientific Research (FNRS). Funding for this research was managed by the PRODEX program of the European Space

Agency in collaboration with the Belgian Science Policy Office and by FRFC grant #2.4541.11. The authors thank the reviewer for helpful comments.

References

Ajello, J.M., 1971 a. Emission Cross Sections of CO by Electron Impact in the Interval 1260-5000 Å . I, J. Chem. Phys., 55, 3158-3168.

Ajello, J.M., 1971 b. Emission Cross Sections of CO_2 by Electron Impact in the Interval 1260-4500 Å. II, 55, 3169-3177.

Broadfoot, A.L., Kumar, S., Belton, M.J.S., McElroy, M.B., 1974. Ultraviolet Observations of Venus from Mariner 10: Preliminary Result. Science 183, 1315-1318.

Curdt, W., Brekke, P., Feldman, U., Wilhelm, K., Dwivedi, B.N., Schühle, U., Lemaire, P., 2001. The SUMER spectral atlas of solar-disk features, A&A 375, 591-613, doi: 10.1051/0004-6361:20010364.

Dunseath, K.M., Fon, W. C., Burke, V. M;, Reid, R.H.G. Noble, C.J., 1997. Electron-impact excitation of the n ≤ 4 levels of carbon, J. Phys B: At. Mol. Opt. Phys., 30, 277–287.

Esposito, L.W., J.E. Colwell, W.E. McClintock, 1998. Cassini UVIS observations of Saturn rings, Planet. Space. Sci. 46, 1221-1235, doi:10.1016/S0032-0633(98)00076-2.

Feldman, P.D., Burgh E.B., Durrance S.T., Davidsen A.F., 2000. Far-ultraviolet spectroscopy of Venus and Mars at 4 Å resolution with the Hopkins Ultraviolet Telescope on ASTRO-2. Astrophys. J. 538, 395- 400, doi: 10.1086/309125.

Fox, J.L., 1982. Atomic carbon in the atmosphere of Venus, J. Geophys. Res., 87, 9211–9216.

Fox, J.L., 2003. Effect of H_2 on the Martian ionosphere: Implications for atmospheric evolution. J. Geophys. Res., 108(A6), 1223, doi:10.1029/2001JA000203.

Fox, J.L., Bakalian, F.M., 2001. Photochemical escape of atomic carbon from Mars. J. Geophys. Res., 106, 28,785– 28,791.

Fox, J.L., Bougher, S.W., 1991. Structure, Luminosity, and Dynamics of the Venus Thermosphere, Space Sci. Rev., 55, 357-489.

Fox, J.L., Dalgarno, A., 1981. Ionization, luminosity, and heating of the upper atmosphere of Venus. J. Geophys. Res., 86, 629–639.

Fox, J.L. Paxton, L.J., 2005. C and C^+ in the Venusian thermosphere/ionosphere. J. Geophys. Res., 110, A01311, doi:10.1029/2004JA010813.

Fox, J.L., Sung, K.Y., 2001. Solar activity variations in the Venus thermosphere/ionosphere. J. Geophys. Res., 106, 21,305– 21,335.

Froese Fischer, C., 2006. Some improved transition probabilities for neutral carbon, J. Phys. B, 39, 2159–2167, doi:10.1088/0953-4075/39/9/005.

Gérard, J.-C., Gustin, J., Hubert, B., Gladstone, G.R., Esposito L.W., 2011. Measurements of the helium 584 Å airglow during the Cassini flyby of Venus. Planet. Space Sci., 59, 1524–1528.

Gérard, J.-C., Hubert, B., Shematovich, V.I., Bisikalo, D.V., Gladstone, G.R., 2008. The Venus ultraviolet oxygen dayglow and aurora: Model comparison with observations. Planet. Space Sci. 56, 542–552, doi:10.1016/j.pss.2007.11.008.

Gladstone, G.R., 1985. Radiative transfer of resonance lines with internal sources. J. Quant. Spectrosc. Radiat. Trans. 33, 453–458.

Gladstone, G.R., 1992. Solar OI 1304 Å triplet line profiles. J. Geophys. Res. 97, 19519-19525.

Golbach, C. Nollez, G., 1987. Oscillator strength measurements in the vacuum-ultraviolet. II - The strong 1260, 1277, 1329, 1463, 1561, and 1657 Å multiplets of neutral carbon. Astron. Astrophys., 181, 203 – 209.

Hubert, B., Gérard, J.-C., Gustin, J., Shematovich, V.I., Bisikalo, D.V., Stewart, A.I., Gladstone, G.R., 2010. UVIS observations of the FUV OI and CO 4P Venus dayglow during the Cassini flyby. Icarus, 207, 549-557, doi 10.1016/j.icarus.2009.12.029.

Krasnopolsky, V.A., Parshev, V.A., 1983. Photochemistry of the Venus atmosphere. In: Hunten, D.M., Colin, L., Donahue, T.M., Moroz, V.I. (eds), Venus. Univ. of Arizona Press, Tucson, USA, pp 431-458.

Nir S., Adams, S., Rein, R., 1973. Polarizability calculations on water, hydrogen, oxygen, and carbon dioxide, J. Chem. Phys., 59, 3341 – 3455.

Paxton, L.J., 1983. Atomic carbon in the Venus thermosphere: Observations and theory, Ph.D. thesis, University of Colorado, Boulder, Colo.

Paxton, L.J., 1985. Pioneer Venus Orbiter Ultraviolet Spectrometer limb observations: Analysis and interpretation of the 166- and 156-nm data. J. Geophys. Res., 90, 5089–5096.

Reader, J., Corliss, C.H., Wiese C.L., Martin, G.A., 1980. Wavelengths and Transition Probabilities for Atoms and Atomic Ions, Part. I. Wavelengths, Part II. Transition Probabilities, Nat. Stand. Ref. Data Ser., NSRDS-NBS 68, U.S. Government Printing Office, Washington, D.C.

Richards, P.G., Fennelly, J.A., Torr, D.G., 1994. EUVAC: a solar EUV flux model for aeronomic calculations. J. Geophys. Res. 99, 8981–8992, doi:10.1029/ 94JA00518.

Rottman, G.J., Moos, H.W., 1973. The ultraviolet (1200 – 1900 Å) spectrum of Venus. J. Geophys. Res., 78, 8033 - 8048.

Shematovich, V.I., Bisikalo, D.V., Gérard, J.-C., Cox, C., Bougher, S.W., Leblanc, F., 2008. Monte Carlo model of the electron transport for the calculations of Mars dayglow emissions. J. Geophys. Res. 113, E02011, doi:10.1029/2007JE002938.

Shine, R.A., Bruce, W.L., Chipman, E.G., 1978. Overlapping emission peaks in the solar CI multiplets at λ1650 and λ1657, Astrophys. J., 224, 247-258.

Shirai, T., Tabata, T., Tawara, H., 2001. Analytic cross sections for electron collisions with CO, CO_2, and H_2O relevant to edge plasma impurities, At. Data Nucl. Data Tables, 79, 143 – 184.

Stewart, A.I., Anderson, D.E., Esposito, L.W., Barth, C.A., 1979. Ultraviolet spectroscopy of Venus: Initial results from the Pioneer Venus Orbiter. Science, 203, 777– 779.

Thomas, G.E., Stamnes, K., 1999. Radiative transfer in the Atmosphere and Ocean, Cambridge University Press, Cambridge, UK, page 73.

Woods, T.N., Bailey, S.M., Eparvier, F.G., Lawrence, G.M., Lean, J., McClintock, W.E., Roble, R.G., Rottman, G.J., Solomon, S.C., Tobiska, W.K., White, O.R., 2000. The TIMED solar EUV experiment, Phys. Chem. Earth Pt. C, 25, 5-6, 393-396, doi:10.1016/S1464-1917(00)00040-4.

Wiese, W. L., Fuhr, J. R., 2007, Improved Critical Compilations of Selected Atomic Transition Probabilities for Neutral and Singly Ionized Carbon and Nitrogen, J. Phys. Chem. Ref. Data, 36, 1287-1345.

Woods, T., Rottman, G., 2002. Solar ultraviolet variability over time periods of aeronomic interest, atmospheres in the solar system: comparative aeronomy. In: Mendillo, M., Nagy, A., Waite, J.H. (Eds.), Geophysical Monograph 130. American Geophysical Union, Washington, DC, p. 221 - 234.

Wu, C.Y.R., and Judge, D.L., 1981. Atomic carbon emission produced through photodissociative excitation of CO, J. Chem. Phys., 75, 2826-2830.

Wu, C.Y.R, Phillips, E., Lee, D.L., Judge, C.L., 1978. Atomic carbon emission from photodissociation of CO_2, J. Geophys. Res., 83, 4869-4872.

Tables

Emission (upper and lower state)	Wavelength (nm)
CO (A $\rightarrow$ X) Fourth positive system	130 - 200
OI ($2s^2 2p^3 (^4S°) 3s\ ^3S^o \rightarrow 2s^2 2p^4\ ^3P$)	130.4
OI ($2s^2 2p^3 (^4S°)\ 3s\ ^5S^o \rightarrow 2s^2 2p^4\ ^3P$)	135.6
CI ($2s^2 2p\ 3d\ ^3P^o \rightarrow 2s^2 2p^2\ ^3P$)	126.1
CI ($2s^2 2p3d\ ^3D^o \rightarrow 2s^2 2p^{2\ 3}P$)	127.8
CI ($2s2p^3\ ^3P^o \rightarrow 2s^2 2p^2\ ^3P$)	132.9
CI ($2s2p^2 (^4P) 3s\ ^5P \rightarrow 2s2p^3\ ^5S^0$)	143.2
CI ($2s^2 2p3d\ ^1F^o \rightarrow 2p^2\ ^1D$)	146.3
CI ($2s2p^3\ ^3D^o \rightarrow 2s^2 2p^2\ ^3P$)	156.1
CI ($2s^2 2p3s\ ^3P^o \rightarrow 2s^2 2p^2\ ^3P$)	165.7
CII ($2s2p^2\ ^2D \rightarrow 2s^2 2p\ ^2P^o$)	133.5

Table 1. List of emissions explicitly included in the fitting procedure of the UVIS spectra between 125 and 180 nm.

Multiplet	λ_{min} (nm)	λ_{max} (nm)	Relative contribution
CI ($2s^22p\ 3d\ ^3P^o \rightarrow 2s^22p^2\ ^3P$)	125	129	0.018
CI ($2s2p^3\ ^3D^o \rightarrow 2s^22p^2\ ^3P$)	152	160	0.0508
CI ($2s^22p3s\ ^3P^o \rightarrow 2s^22p^2\ ^3P$)	163	168	0.109

Table 2. Relative contribution of the CI multiplets to the solar flux in wavelength intervals determined by λ_{min} and λ_{max} allowing to estimate the CI multiplet fluxes from low resolution solar spectra.

Transition	λ(nm)	A_{ul} (10^7 s^{-1})	x_{diss} (sdu)	x_{off} (sdu)	σ_{CO_2} (10^{-20} cm^{-2})	$F_\odot$ (ph cm^{-2} s^{-1})
$^3P_1$-$^3P_0$	165.7907	34.7	13.259	11.514	6.57	
$^3P_1$-$^3P_2$	165.6267	8.72	13.200	13.696	6.79	
$^3P_2$-$^3P_2$	165.7008	26.1	13.400	12.526	6.69	1.89×10^{10}
$^3P_0$-$^3P_1$	165.6929	11.6	13.742	10.642	6.70	
$^3P_1$-$^3P_1$	165.7379	8.66	20.384	17.545	6.64	
$^3P_2$-$^3P_1$	165.8121	14.4	20.612	20.361	6.54	
$^3P_2$-$^3D_3$	156.1438	11.7	11.611	13.341	30	
$^3P_1$-$^3D_2$	156.0682	8.82	12.046	13.305	30	
$^3P_2$-$^3D_2$	156.1340	2.93	12.126	12.871	30	6.37×10^9
$^3P_0$-$^3D_1$	156.0309	6.54	13.118	13.883	30	
$^3P_1$-$^3D_1$	156.0709	4.89	11.719	12.986	30	
$^3P_2$-$^3D_1$	156.1367	0.325	11.966	13.656	30	
$^3P_1$-$^3P_0$	126.0927	18.1	14.015	13.861	29.7	
$^3P_1$-$^3P_2$	126.1122	4.0	14.015	13.861	29.9	
$^3P_2$-$^3P_2$	126.1552	13.4	14.015	13.861	30.2	1.57×10^8
$^3P_0$-$^3P_1$	126.0735	5.70	14.015	13.861	29.6	
$^3P_1$-$^3P_1$	126.0996	4.68	14.015	13.861	29.8	
$^3P_2$-$^3P_1$	126.1426	7.51	14.015	13.861	30.1	

Table 3. Atomic parameters and solar fluxes used in the modeling of the CI multiplets at 126.1, 156.1 and 165.7 nm. The Einstein coefficients A_{ul} are all very large, so that optical thickness can become large, even at rather low carbon densities. The solar flux $F_\odot$is given for the total sextuplets, at 1 AU. The parameters of the Gaussian functions are given in standard Doppler units at a reference temperature of 500 K, suitable for the Venus thermosphere. The Rayleigh scattering cross section σ_{CO_2} is computed using the polarizability of Nir et al. (1973). The transition parameters are from Weise and Fuhr (2007).

	126.1 nm	156.1 nm	165.7 nm
Solar (cm^{-2} s^{-1})	3.17×10^5	6.42×10^7	1.60×10^8
Photochemical (cm^{-2} s^{-1})	4.8×10^6	2.03×10^7	4.17×10^7
ratio	0.07	3.16	3.84

Table 4. Column-integrated sources of photons of the CI 126.1, 156.1 and 165.7 nm multiplets in the Venus thermosphere, calculated for the observing conditions of the Cassini-UVIS record 25. The solar source comes from the resonance scattering of the solar photons, photochemical sources include the thermal and non-thermal emissions, and the last line gives the ratio of these two

Figures and captions

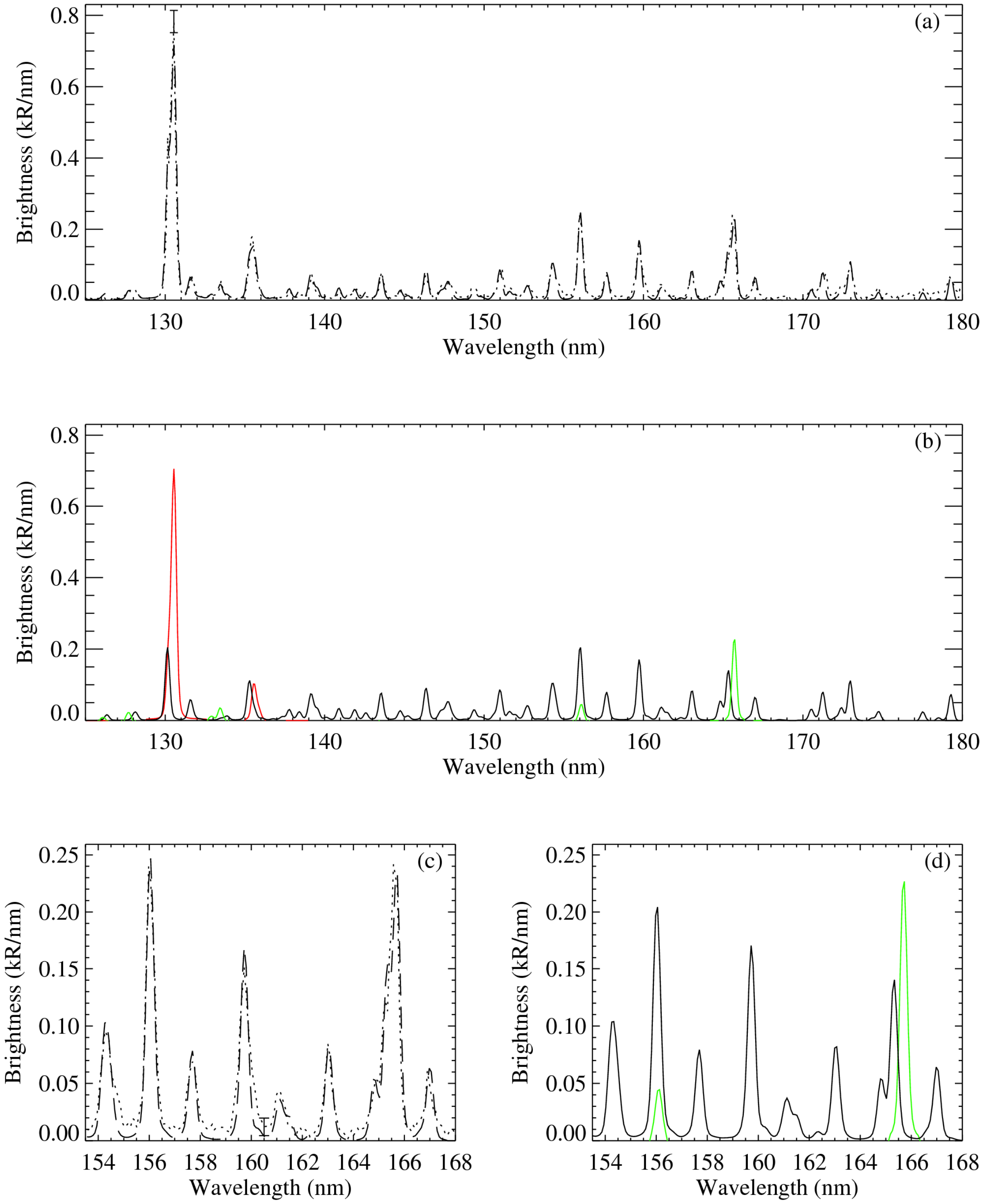

Figure 1. Observed (dotted lines) and fitted (dashed lines) UVIS spectrum obtained with a minimum possible emission angle (Pannel a). Pannel b shows the contributions of the fitted CO-4P bands (black), OI (red) and CI (green) multiplets to the total fitted spectrum. The bright CI multiplets at 156.1 and 165.7 nm are well separated from the surrounding CO-4P spectral features, as it can be seen in panels c and d showing a zoom of panels a and b respectively, on the wavelength interval that contains the brightest CI transitions. The $\pm 2\sigma$ error bars of the brightest feature (the 130.4 nm oxygen multiplet) and of the signal nearby the carbon emissions are also shown.

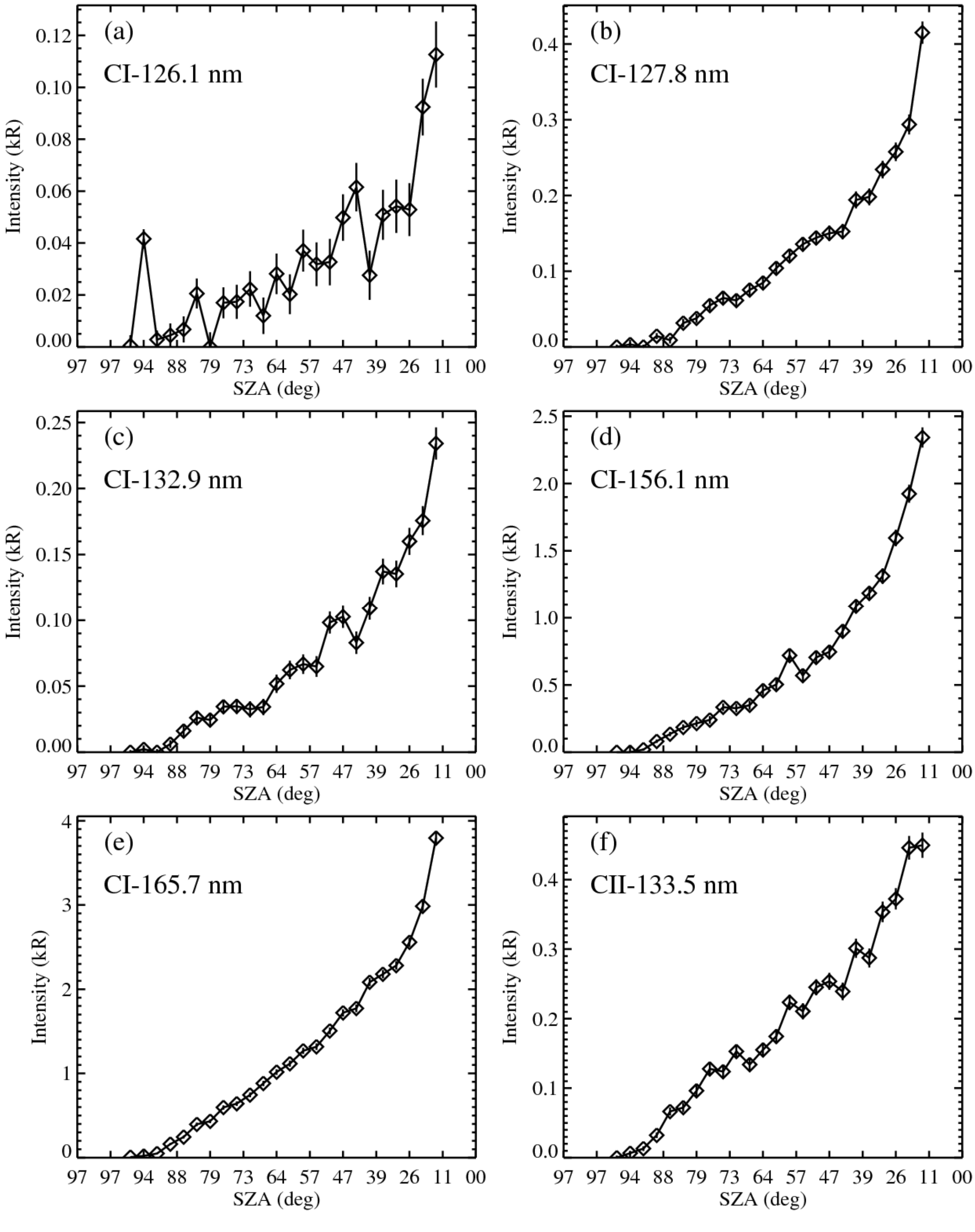

Figure 2. Intensities of the brightest CI (at 126.1 -a-, 127.8 -b-, 132.9 -c-, 156.1 -d- and 165.7 -e- nm) and CII (at 133.5 nm -f-) FUV multiplets recorded between ~125 and 180 nm along the Cassini-UVIS track, plotted versus the solar zenith angle of the emitting layer observed by UVIS. Cassini crossed the morning terminator (SZA~90°) and moved towards the planetary bright limb where larger intensities are recorded.

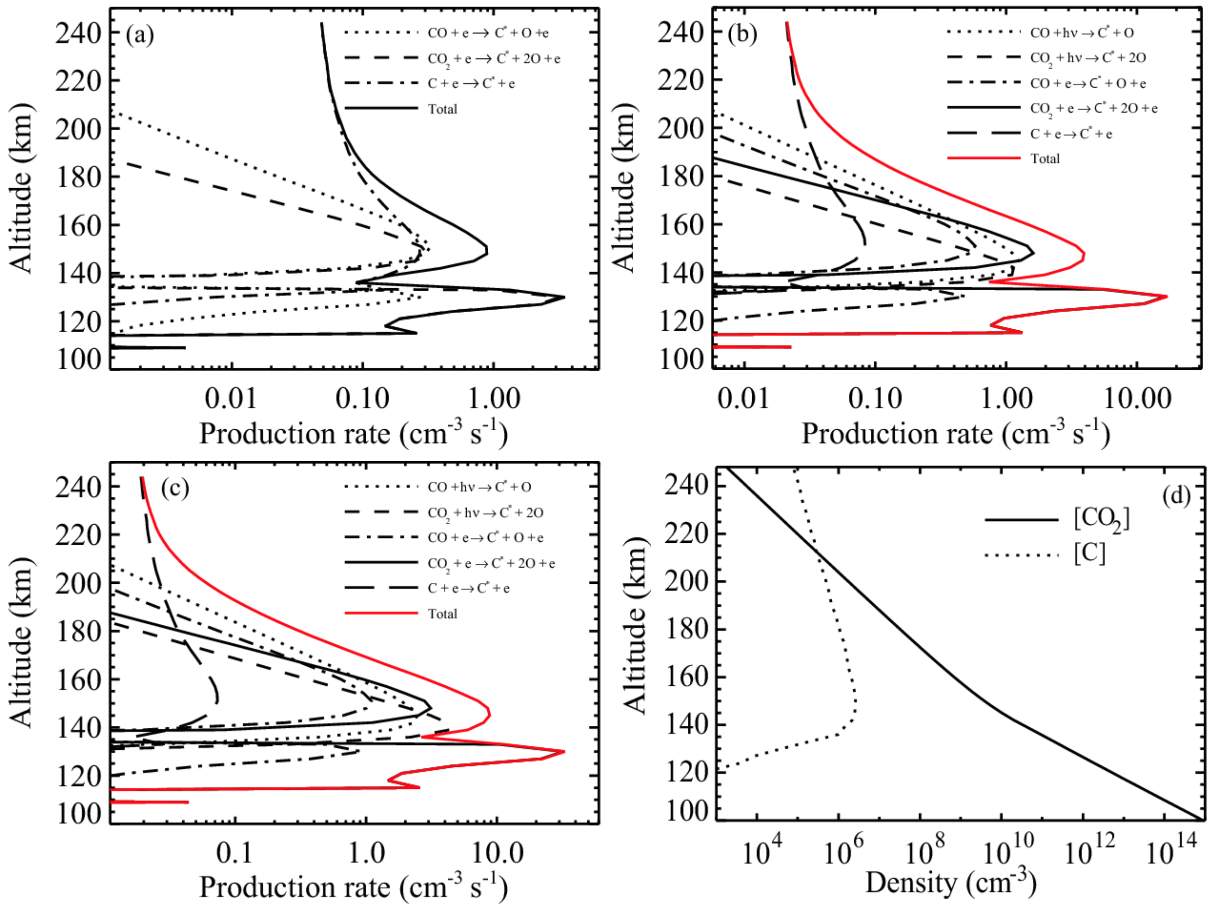

Figure 3. Photochemical production rates of the upper state of the CI 126.1 nm (a), CI 156.1 nm (b) and CI 165.7 nm (c) transitions, computed for the observing conditions of UVIS record 25. TheVTS-3 CO_2 and reference C density profiles adopted in the model are shown in panel (d).

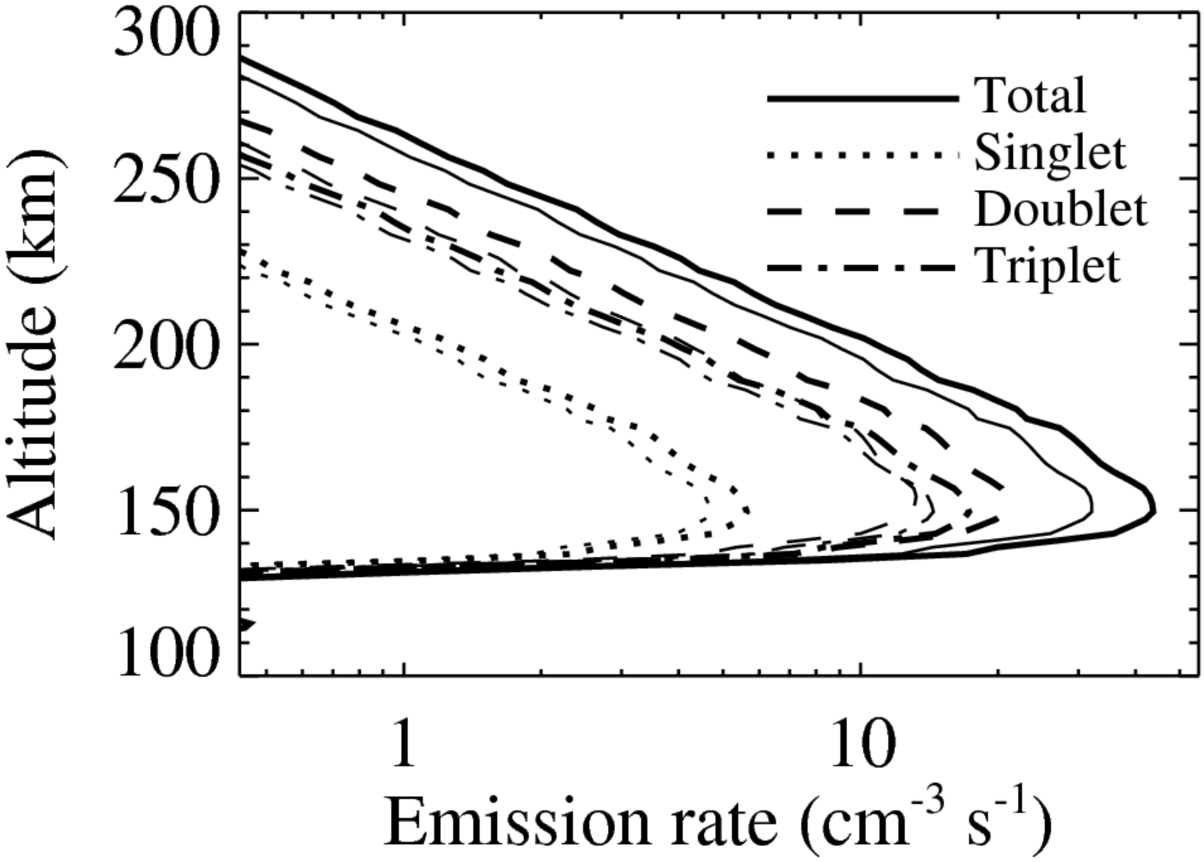

Figure 4. Primary source and RT source function of the CI-165.7 nm multiplet, computed for the observing conditions of Cassini-UVIS record 25, resulting from resonance scattering of sunlight. Thin lines represent the primary sources, thick lines the RT source functions. The multiplet is decomposed into three components, grouping lines having the same upper state (which are added together in this figure), i.e. a singlet, a doublet and a triplet of lines.

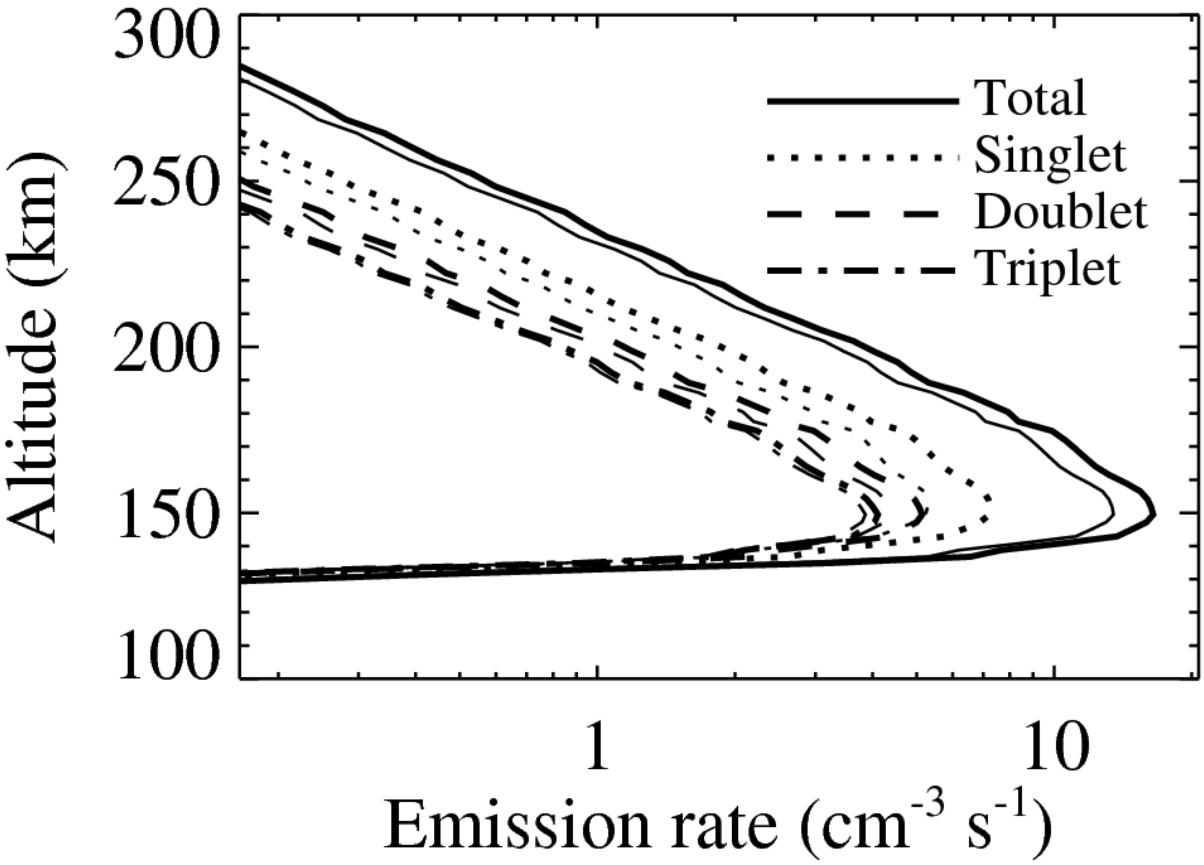

Figure 5. Primary source and RT source function of the CI-156.1 nm multiplet, computed for the observing conditions of Cassini-UVIS record 25, resulting from the scattering of the solar light. Thin lines represent the primary sources, thick lines the RT source functions. The multiplet is decomposed into three components, grouping lines having the same upper state (which are added together in this figure), i.e. a singlet, a doublet and a triplet of lines.

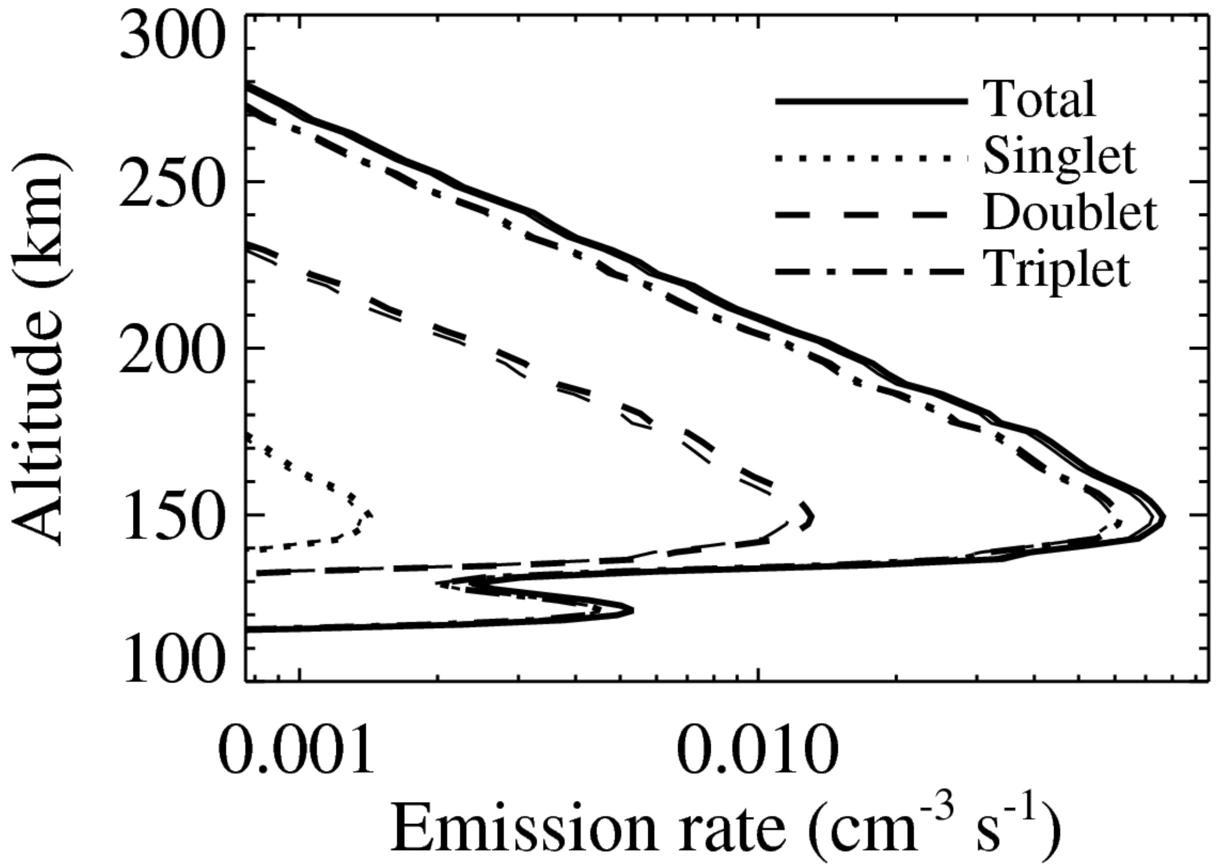

Figure 6. Primary source and RT source function of the CI-126.1 nm multiplet, calculated for the observing conditions of Cassini-UVIS record 25, resulting from the scattering of the solar light. Thin lines represent the primary sources, thick lines the RT source functions. The multiplet is decomposed into three components, grouping lines having the same upper state (which are added together in this figure), i.e. a singlet, a doublet and a triplet of lines.

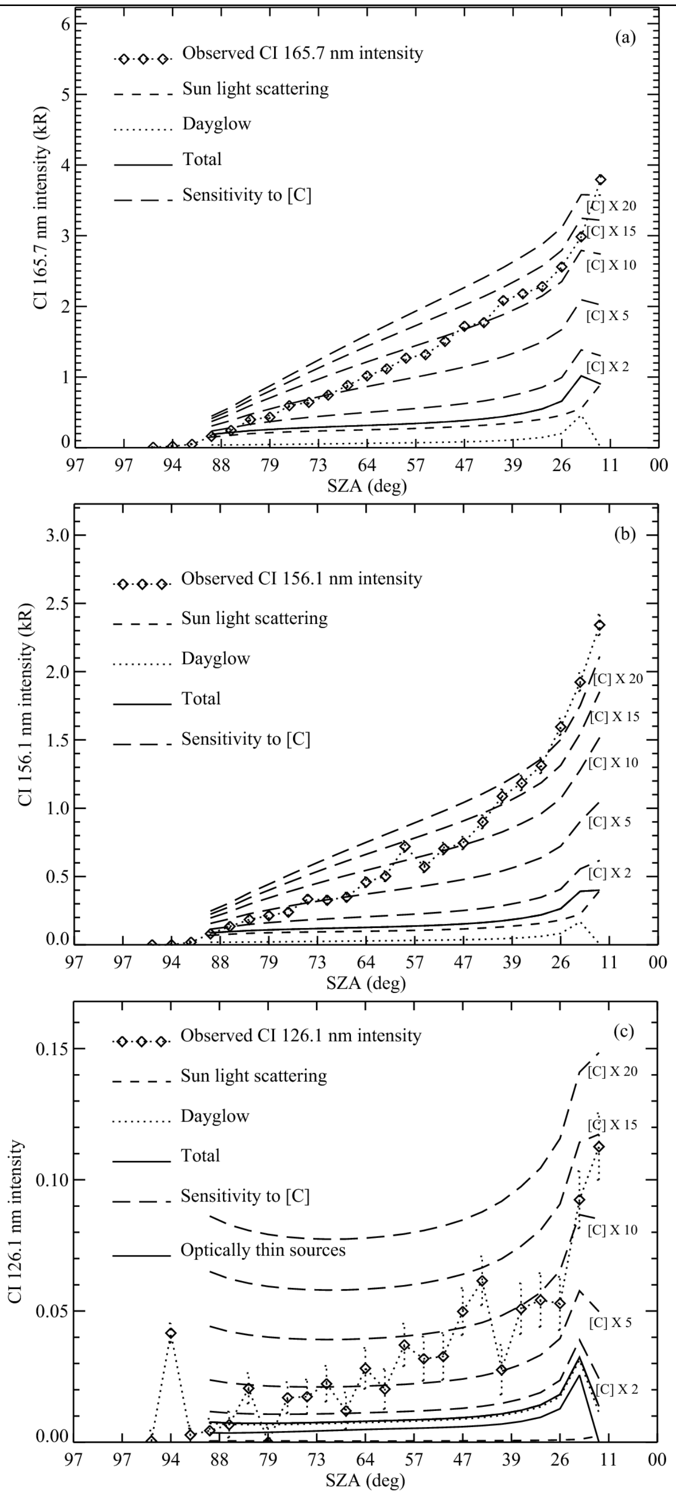

Figure 7. Observed (diamonds) and calculated (solid line) intensity of the CI-165.7 (a), 156.1 (b) and 126.1 (c) nm multiplets, along the Cassini track. Calculations have been carried out for the Cassini-UVIS conditions using the carbon density profile of *Fox and Paxton* (2005). The total 165.7 and 156.1 nm intensity (solid line) is dominated by the contribution of the resonance scattering of sunlight (short dashes) which dominates that of the photochemical sources (dotted lines). The CI-126.1 nm intensity is dominated by the non-thermal photochemical sources, which are optically thin sources (dash-dot-dot, panel c). The sensitivity of the computed intensities versus the carbon density is illustrated by the long dashes, obtained for several scaling factors applied to the original carbon density profile.

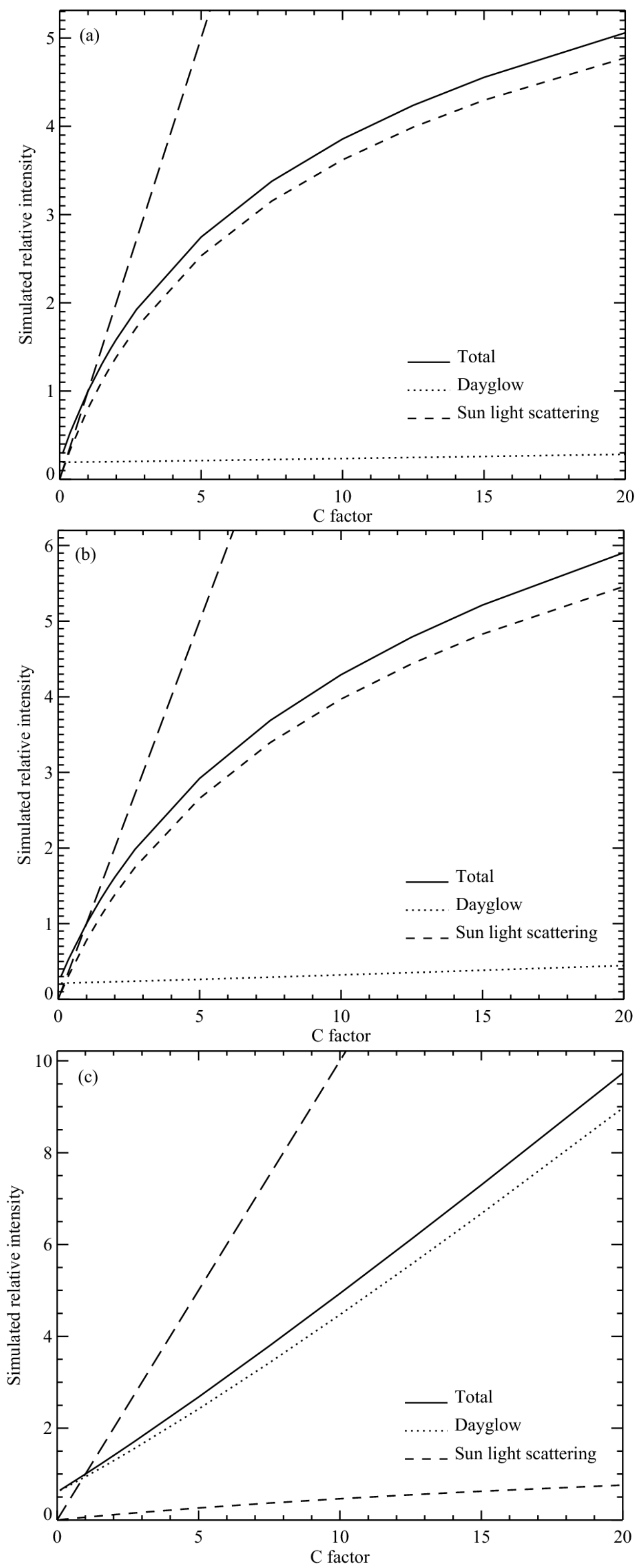

Figure 8. Sensitivity of the calculated intensity of the CI-165.7 (a), 156.1 (b) and 126.1 (c) nm multiplets versus the correction factor applied to the carbon density profile, for the observing conditions of Cassini-UVIS record 25.

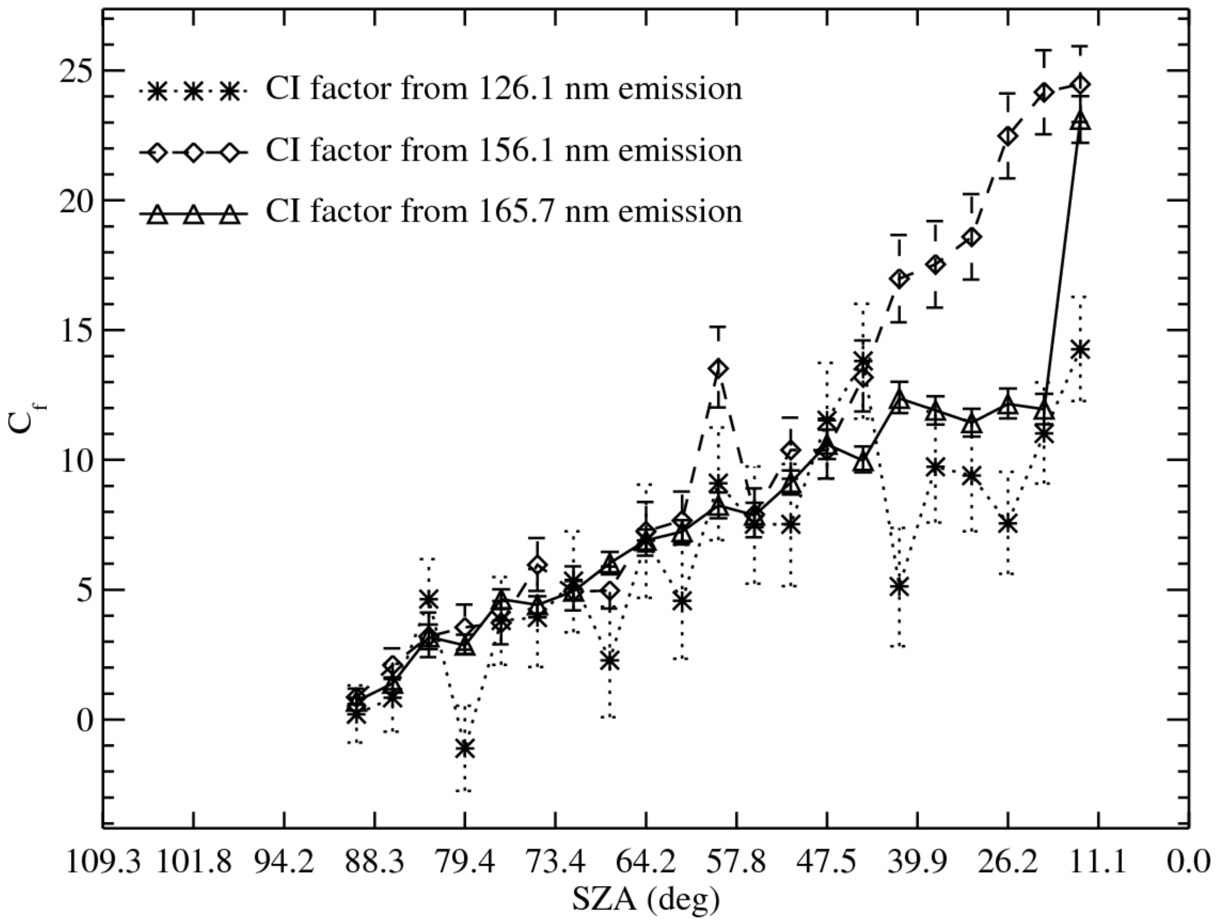

Figure 9. Carbon density scaling factor estimated along the Cassini track from the UVIS observation and modeling of CI-165.7, 156.1 and 126.1 nm multiplets. Calculations conducted for limb conditions (near SZA = 0) may be unreliable. The error bars represent 1-σ uncertainties obtained using the sensitivity of the computed intensities versus the carbon density and the errors on the measured intensities, including the Poisson noise and the chi-square flatness of the fitting process used to estimate the CI multiplets intensities.

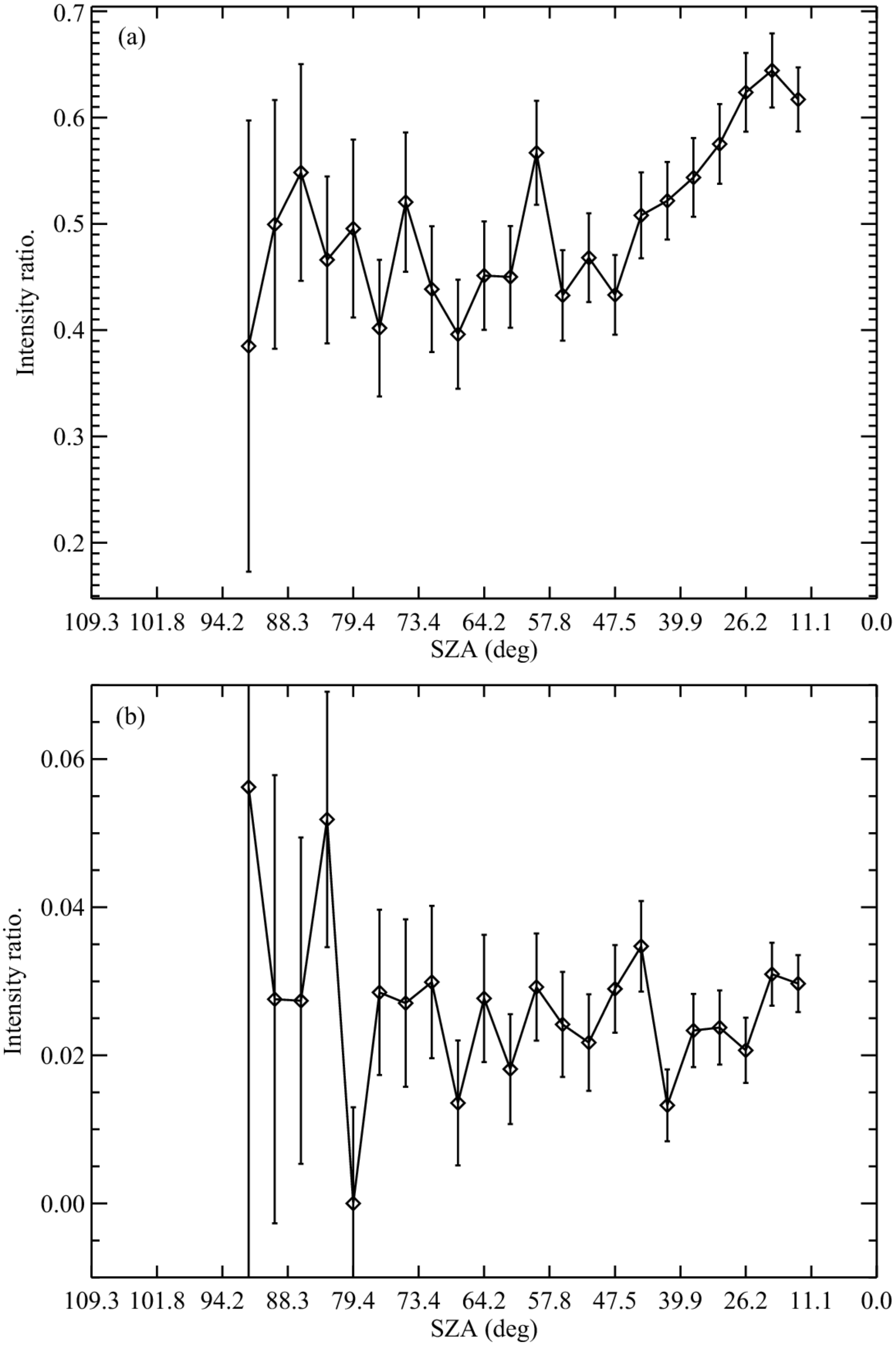

Figure 10. Ratio of the observed Cassini-UVIS CI-156.1 nm (a) and CI-126.1 nm intensity over the CI-165.7 nm intensity observed along the UVIS foot track

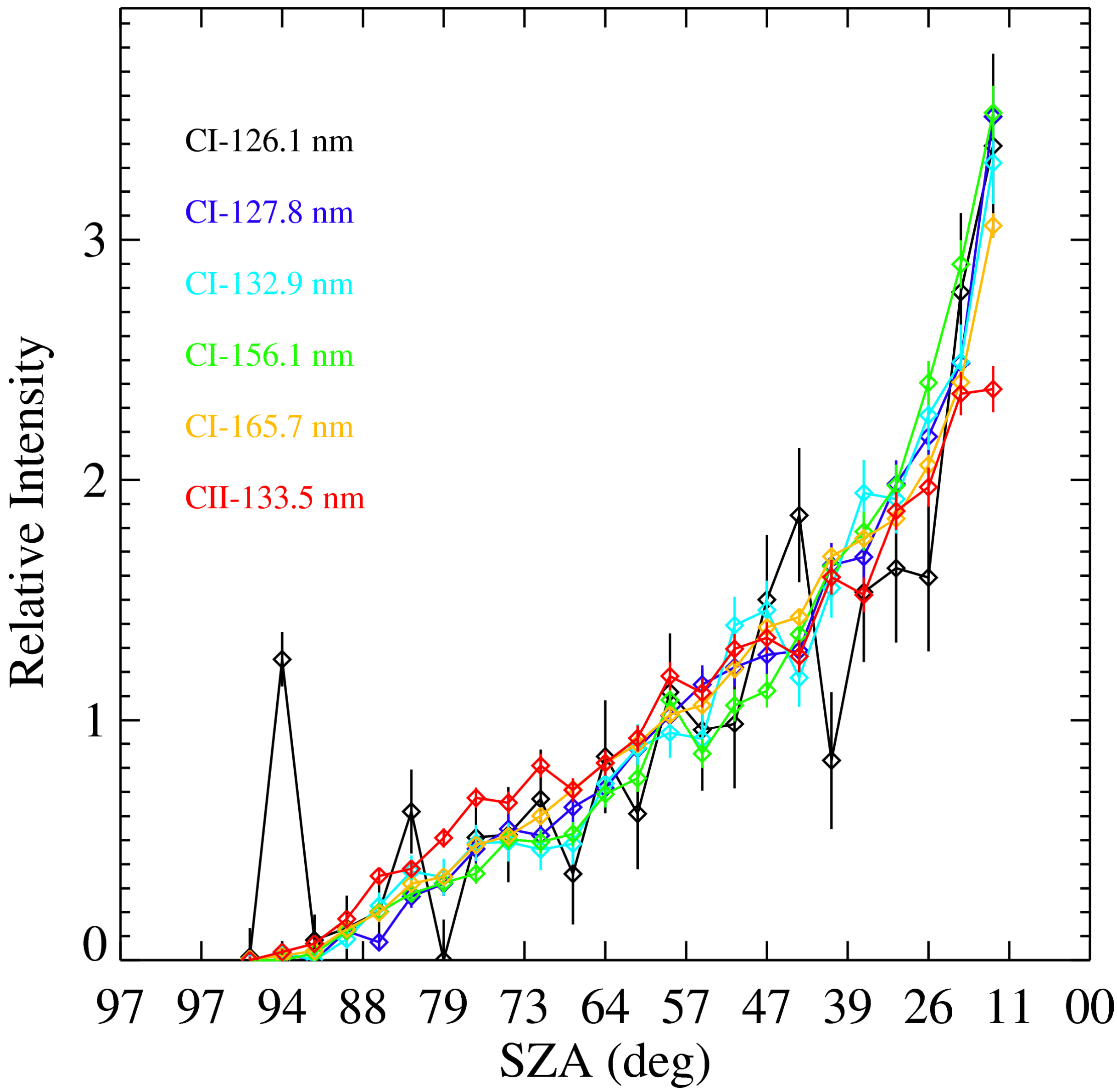

Figure 11. Relative intensity of the emissions shown in **Figure 2**, along the Cassini track. The relative intensities are computed by dividing each curve of **Figure 2** by its average value along the Cassini track.